Rev. Roum. Sci. Techn.– Électrotechn. et Énerg.
Vol. **67**, *3*, pp. 359–365, Bucarest, 2022

A WIRELESS POWER TRANSFER SYSTEM DESIGN USING TRANSMITTER LARGER THAN RECEIVER FOR MOBILE PHONES

ALI AĞÇAL[1], OĞUZHAN VURAL[2]

Keywords: Wireless power transfer; Inductive coupling; Mobile phone; Efficiency; Coupling factor.

In a world where technology grows rapidly, electrical energy is of vital importance. In the recent future, the wireless transmission of electrical energy is expected to play a vital role in our lives. This paper investigated a Wireless Power Transfer (WPT) system with a transmitter size larger than the receiver size. Magnetic resonance coupling was used as the WPT system. Wireless charging of mobile phones was realized with a large transmitter coil and a small receiver coil placed on the back of the mobile phone. In this study, the WPT system was designed for a frequency of 1 MHz and a power of 5 W. As a result of the calculations and simulations made for the WPT system, an efficiency of 97 % was obtained in a 10 mm air gap. Analyzes were made according to the different receiver and transmitter coil sizes and air gaps. The optimal coil size has been determined. Air gap and misalignment limits are determined for optimal coil size. The analytical calculations and modeling of the design are made for the best efficiency and the most suitable receiver and transmitter coil design in Serial-Series (SS) topology. Wireless phone charging design was carried out using various programs. In addition, the effects of the design on human health were examined.

1. **INTRODUCTION**

For centuries, the use of cables in energy transmission has caused serious problems such as cable complexity, visual pollution, limited movement area, water resistance, and cost. In 1891, as an alternative to the cables, Nikola Tesla introduced the idea of wireless energy transmission [1]. Ever Since Tesla, scientists have used various methods such as microwave [2], laser [3], inductive coupling [4], and capacitive coupling [5] as the means of WPT over long distances. Among these methods, Magnetic Resonance Coupling (MRC) is currently deemed the most efficient and commonly used method in the literature. MRC first started in 2007 when it succeeded in lighting a 60 W lamp with wireless energy transfer at 40 % efficiency [6], creating an excellent foundation for the development of the WPT. Nowadays, energy can be transferred with more than 95 % efficiency in the WPT.

In the WPT systems, there is no physical connection element between the source and the load. In magnetic resonance coupling and inductive coupling, energy is transferred between the receiving and transmitting coils through a magnetic field. In magnetic resonance coupled WPT systems, the receiver and transmitter must oscillate at a suitable resonance frequency to transfer the energy transfer with maximum efficiency. It has been shown by Tesla that magnetic resonance directly affects the efficiency of power transfer [1]. The operation of the WPT system in different air gaps also creates a variability of efficiency. Neuman's formula was used to show the relationship between air gap change and efficiency [7]. In addition, in another study, the efficiency equation of the WPT system is obtained with the S parameter, and the algorithm that calculates the s parameter is presented [8]. WPT devices should be designed by considering features such as desired power, efficiency, and usage area. For WPT systems that operate in a high air gap, the transmitter and receiver coil should be designed in a large size [9]. Designing the receiver coil of mobile devices should be kept smaller than the mobile device so that it does not adversely affect daily use. High frequencies should be preferred for better energy transmission due to dimensions [10]. The rectangular structure of the mobile phones and the magnetic flux being concentrated at the corner points of the coil create some difficulties in coil design, causing yield loss. To prevent these losses, the coil design should be oval [11]. Designing the receiver size slightly lower than the transmitter size for high misalignment tolerance is important not only for circular spiral coils but also for hexagonal [12], square [13], and DD structures [14].

In this study, SS compensated WPT system operating with high efficiency up to 13.2 mm air gap at 5 W power was designed for mobile phones. The appropriate design parameters for the WPT system were determined, and mathematical calculations were made to obtain the highest efficiency. As a result of the calculated values, the coil design of the circuit was made. The equivalent circuit of the magnetic resonance coupling system was established, and simulations were carried out using MATLAB/Simulink and ANSYS Maxwell package programs. In addition, the exposure limits specified by the guidelines and standards for protecting human health were compared with the simulation results.

2. **WPT SYSTEM WITH MAGNETIC RESONANCE COUPLING**

In this section, the theory of the WPT system over simple equivalent circuits is explained. The basic series RLC circuit is shown in Fig 1.

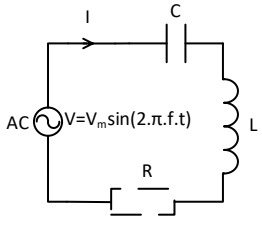

Fig. 1 – Basic series RLC circuit.

In this circuit, *C* is the capacitance of the capacitor, *L* is the inductance of the coil, *R* is the internal resistance of the circuit; f is the frequency of the ax voltage source, and V is the voltage of the ac source. In the series RLC circuit, the frequency at which the inductive reactance of the inductor equals the capacitive reactance of the capacitor is the resonant frequency. Using eq. (1), the resonant frequency of

[1] Suleyman Demirel University, Electrical and Electronics Engineering Department, Isparta, Turkey, E-mail: aliagcal@sdu.edu.tr

the equivalent circuit is found.

$$f = \frac{1}{2\pi\sqrt{LC}}. \quad (1)$$

The capacitance of the resonant capacitor, depending on the operating frequency and the inductance value, is found by:

$$C = \frac{1}{L(2\pi f)^2}. \quad (2)$$

The quality factor of the circuit is as in

$$Q = \sqrt{\frac{L}{C}}\frac{1}{R} = \frac{\omega_0 L}{R}. \quad (3)$$

The inductance value of the circuit, depending on the operating frequency, quality factor, and internal resistance values, is found by eq. (4).

$$L_1 = L_2 = \frac{QR}{2\pi f}. \quad (4)$$

If two of the resonator circuits in Fig. 1 are placed opposite to each other with a certain air gap, the magnetic connection occurs between the transmitter and receiver coils. Consequently, the resonator circuit in Fig. 2 is formed.

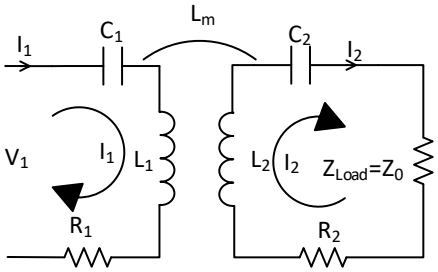

Fig. 2 – Magnetic resonance coupling circuit.

V_1 is the input voltage of the WPT system. Respectively, C_1 and C_2 are the transmitter and receiver resonance capacitors, L_m is the mutual inductance, L_1 and L_2 are the transmitter and receiver coils inductances, Z_0 is the output load, R_1 and R_2 are the receiver and transmitter coil's internal resistance, respectively. The efficiency of the WPT system varies according to the resonators and the coupling factor (k) between them. The mutual inductance between opposing coils is calculated by:

$$L_m = k\sqrt{L_1 L_2}. \quad (5)$$

The ratio between output and input current is as in [15]:

$$\frac{I_2}{I_1} = \frac{j\omega L_m}{j\omega L_2 + \frac{1}{j\omega C_2} + Z_0 + R_2}. \quad (6)$$

The equivalent impedance (Z_{Eq}) of the WPT system is given by [9, 15]:

$$Z_{Eq} = R_1 + j\omega L_1 + \frac{1}{j\omega C_1} + \frac{L_m^2\omega^2}{j\omega L_2 + \frac{1}{j\omega C_2} + Z_0 + R_2}. \quad (7)$$

The efficiency of the WPT system is calculated by [9, 15]:

$$\eta = \left(\frac{j\omega L_m}{j\omega L_2 + \frac{1}{j\omega C_2} + Z_0 + R_2}\right)^2 \times \frac{Z_0}{Z_{Eq}}. \quad (8)$$

In the WPT system, three or one resonance frequency occurs depending on the mutual inductance, load resistance, internal resistance, and natural angular frequency. If the circuit parameters of the WPT system satisfy the condition of eq. (10), in other words, if the air gap between the receiver and the transmitter is lower than the critical air gap, the system has three resonance frequencies. In the cases of eq. (11) where the air gap is higher than the critical air gap, the system has a single resonance frequency. This resonance frequency is equal to the natural frequency. The critical mutual inductance ($L_{mcritical}$) at which frequency bifurcation begins is calculated by [7]:

$$L_{m_{Critical}}^2 = \frac{Z_0^2 - R_2^2}{\omega_0^2}, \quad (9)$$

$$L_m^2 > \frac{Z_0^2 - R_2^2}{\omega_0^2}. \quad (10)$$

$$L_m^2 < \frac{Z_0^2 - R_2^2}{\omega_0^2}. \quad (11)$$

In WPT systems, the resonance frequency starts to bifurcate when it is above the critical mutual inductance value. However, it is desired to keep the system working above this value because the efficiency will be at its maximum. If the system is below the critical mutual inductance value, the efficiency will start to decrease as the mutual inductance decreases.

3. COIL DESIGN AND EQUIVALENT CIRCUIT SIMULATION RESULTS

3.1. SPIRAL COIL DESIGN

In this study, different-sized transmitter and receiver coils were designed for the WPT system. Since the size of the receiver coil is limited by the space of the mobile phone, it is designed to be 5 cm in diameter, and the size of the transmitter coil is 7.5 cm in diameter. The top and side view of spiral inductance is given in Fig. 3.

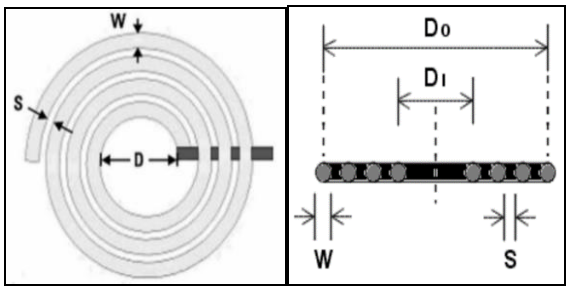

a) b)

Fig. 3 – a) Top; b) side view of spiral inductance.

The inductance of the spiral coil is determined by [16]

$$L = \frac{N^2 A^2}{30A - 11D_i}, \quad (12)$$

$$A = \frac{D_i + N(W+S)}{2}, \quad (13)$$

where W is the diameter of the wire, S is the distance between two wires, and N is the number of turns. Respectively, D_0 and D_I are the outer and inner diameters of spiral coils. Receiver and transmitter coils are designed by eq. (13). The parameters of the receiver and transmitter coil are given in Table 1.

Table 1
Receiver and transmitter coil parameters

Coil location	Receiver	Transmitter
Outer diameter	50 mm	75 mm
Inner diameter	29 mm	60 mm
Number of turns	7	5
Wire thickness	0.75 mm	0.75 mm
Space between wires	0.75 mm	0.75 mm
Wire length	0.87 m	1.06 m
Inductance	2.751 µH	3.17 µH

Coils designed in Ansys Maxwell 3D are shown in Fig. 4.

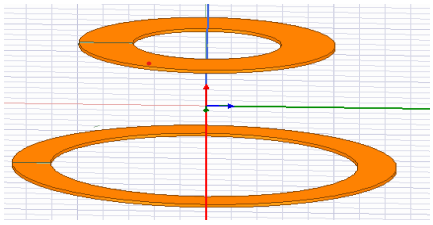

Fig. 4 – Coil design in Ansys Maxwell 3D.

As a result of Maxwell 3D simulation, the receiver coil inductance L_2(Rx) was found to be 2.626 µH, and the transmitter coil inductance L_1(Tx) was found to be 3.170 uH.

3.2 MATLAB/SIMULINK SIMULATION

The WPT circuit set up in the MATLAB/Simulink program is shown in Fig. 5.

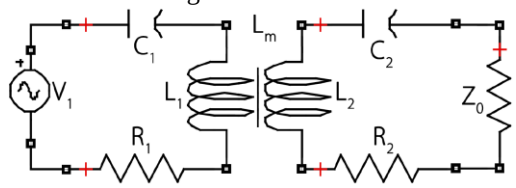

Fig. 5 – WPT circuit in MATLAB/Simulink

Parameters of the WPT circuit are given in Table 2.

Table 2
Circuit parameters of the WPT system

L_1	3.17 µH
L_2	2.626 µH
C_1	7.991 nF
C_2	9.6681 nF
$L_{mcritical}$	632 nH

According to the circuit parameters in Table 2, efficiency-frequency and equivalent impedance-frequency graphs are shown in Fig. 6 and Fig. 7 for 0 mm and 20 mm air gap, respectively.

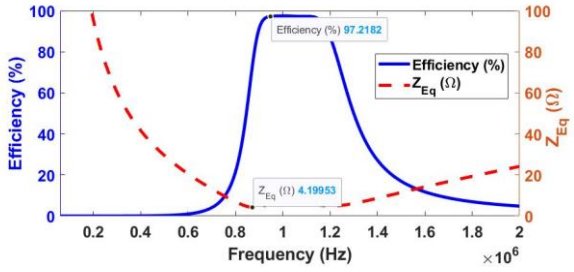

Fig. 6 – Efficiency-frequency graph for 0 mm air gap.

WPT systems with different sizes of receiver and transmitter coils have less frequency bifurcation than those with the same coil sizes. In addition, the frequency range with high efficiency is wider in the WPT systems with different coil sizes. As seen in Fig. 6, frequency bifurcation occurred very little, even below the critical air gap, in this study. Since bifurcation is small, systems with receiver size smaller than transmitter size are well suited for fixed frequency systems.

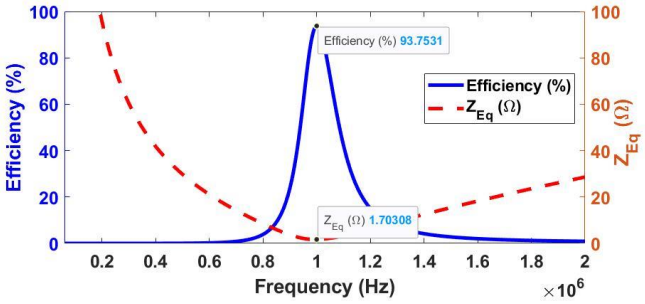

Fig. 7 – Efficiency-frequency graph for 20 mm air gap.

The WPT circuit has been simulated for a 0 mm and 20 mm air gap in MATLAB/Simulink, and the measured values are shown in Table 3.

Table 3
MATLAB/Simulink simulation results

Air gap = 20 mm	Air gap = 0 mm
k = 0.158	k = 0.337
L_m = 456 nH	L_m = 970 nH
V_1 = 3.13 V	V_1 = 6.45 V
I_1 = 1.85 A	I_1 = 0.97 A
I_2 = 1.05 A	I_2 = 1.02 A
f_r = 1 MHz	f_r = 0.9375 MHz
P_1 = 5.290 W	P_1 = 5.132 W
P_2 = 5 W	P_2 = 5 W
η = 94.54 %	η = 97.42 %
V_{C1} = 36.89 V	V_{C1} = 20.7 V
V_{C2} = 17.23 V	V_{C2} = 17.81V

f_r is the resonant frequency, V_{C1} is the transmitter capacitor voltage, V_{C2} is the receiver capacitor voltage, and η is the efficiency. The changing air gap affected the efficiency, equivalent impedance, and resonance frequency values. As a result of the changing coupling factor, it has been observed that the mutual inductance of the circuit and, accordingly, the many operating characters of the circuit have changed.

3.3. ANSYS MAXWELL 3D SIMULATION

As the air gap between the coils and coil sizes change, many parameters change in WPT systems depending on the change of the mutual inductance.

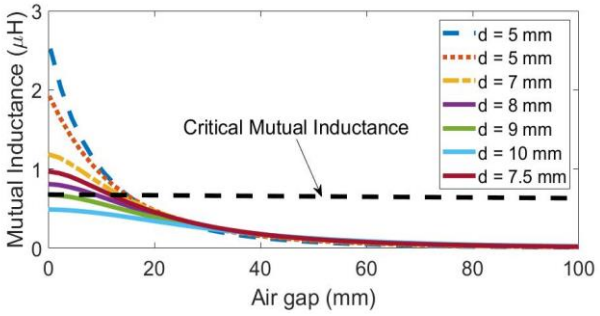

Fig. 8 – Mutual inductance-air gap graph for different transmitter coil sizes in the aligned condition.

The mutual inductance graph according to variation of air gap for fixed receiver and different transmitter sizes is shown in Fig. 8.

Mutual inductance examinations were made for the transmitter coil size of 5 cm, 6 cm, 7 cm, 7.5 cm, 8 cm, 9 cm, and 10 cm by keeping the receiver coil size constant at 5 cm. In the aligned condition, the mutual inductance decreases as the difference between the transmitter and receiver coil sizes increases. In wireless phone charging systems, the user may not always be able to position the receiver and transmitter coil fully aligned. If the coils are designed with the same or similar dimensions, the mutual inductance, and coupling factor values will be high in the aligned condition. However, with small shifts to the right or left, the mutual inductance drops very quickly. The transmitter coil size must be larger than the receiver coil size to minimize misalignment losses. However, if the size differences of the coils are amplified, the mutual inductance and connection factor are seriously reduced, leading to a decrease in efficiency. In this study, the optimum transmitter coil size was determined as 7.5 cm for a 5 cm diameter receiver coil. The critical mutual inductance was calculated as 632 nH by eq. (9). As seen in Fig 8, the air gap corresponding to the critical mutual inductance value for the system with a 75 mm diameter transmitter coil in the aligned position is 13.2 mm. The 13.2 mm air gap is the critical air gap for the system with a 75 mm diameter transmitter.

As the air gap and the size difference of the coils increase in the aligned condition, the coupling factor value (k) decreases. The air gap-coupling factor graph for different coil sizes is given in Fig. 9.

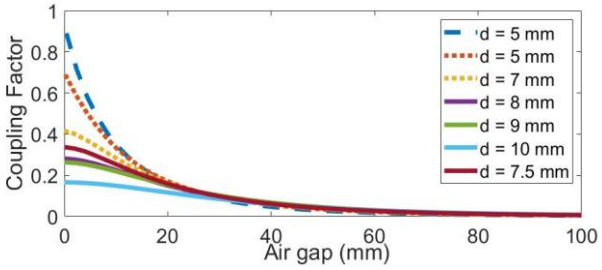

Fig. 9 – Coupling factor-air gap graph for different transmitter coil sizes in the aligned condition.

In the absence of alignment, the effect of different transmitter coil sizes on the mutual inductance was investigated. The WPT system was analyzed by shifting the receiver coil 2 cm on the horizontal axis. The unaligned WPT system designed in Maxwell 3D is shown in Fig. 10.

The coupling factor-air gap graphs for fixed receiver size and different transmitter sizes in the 2 cm unaligned state are shown in Fig. 11. For transmitter and receiver coil sizes close to each other, the mutual inductance and coupling factors are high in the aligned condition and very low in the unaligned condition. In addition, the coupling factor is small in WPT systems with a very large transmitter coil.

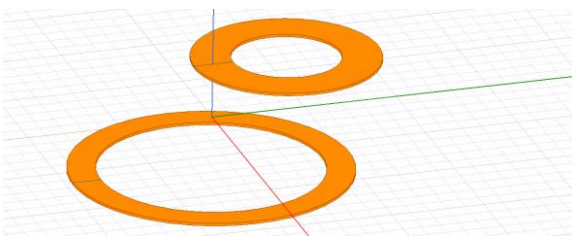

Fig. 10 – Unaligned WPT system in Maxwell 3D.

The 75 mm diameter transmitter coil has the highest coupling factor in the unaligned condition. The 75 mm diameter transmitter coil has the highest coupling factor in the unaligned condition. Therefore, a 75 mm transmitter coil diameter is the most suitable coil size to minimize misalignment losses and maximize efficiency in this study.

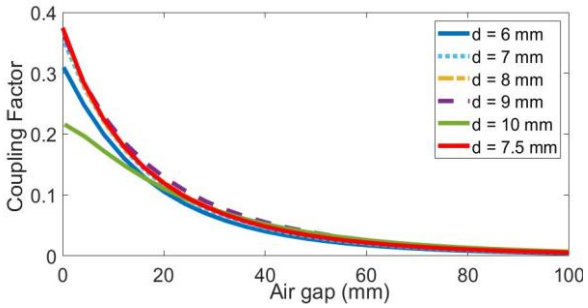

Fig. 11 – Coupling factor-air gap graph according to transmitter coil dimensions in the unaligned condition.

To examine how the efficiency is affected in the case of misalignment in WPT systems used in mobile devices such as phones, a WPT system with a 75 mm transmitter and 5 cm receiver coil dimensions was analyzed according to different misalignments on the horizontal axis. The mutual inductance-air gap graph created by shifting the receiver coil by 0 cm, 1 cm, 2 cm, 3 cm, and 4 cm on the horizontal axis concerning the transmitting coil is given in Fig. 12. The critical air gap values at different misalignment states are shown in Fig. 12.

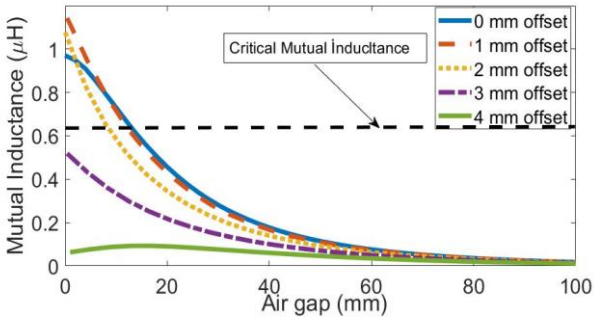

Fig. 12 – Mutual inductance-air gap graph according to different alignment ranges for 75 mm diameter transmitter coil.

The critical air gap of the WPT system in the aligned and unaligned state was determined in Fig. 12. Based on the critical mutual inductance value calculated as 632 nH, the critical air gap is 13.2 mm for the aligned state. In the unaligned state, energy is transferred with maximum efficiency at the air gaps of 12.34 mm and 8.58 mm for 1 cm and 2 cm, respectively. The mutual inductance at 3 cm and 4 cm shift in the unaligned condition is below the critical inductance value. At 3 cm, the efficiency of WPT is low. If the coils are shifted by 4 cm or more, the mutual inductance and coupling factor values are not at a sufficient level for energy transfer. When the aligned and unaligned conditions are examined, the maximum value of the mutual inductance and coupling factor is observed in the 1 cm unaligned condition. In WPT systems with the same transmitter and receiver sizes, the mutual inductance in the unaligned state is lower than in the aligned state. However, for the WPT systems with different receiver and transmitter sizes, the path of the magnetic flux is shorter, the magnetic reluctance is less, and the mutual inductance is higher in the unaligned state than in the aligned state up to a certain slip value. In this WPT design, the mutual inductance of the unaligned state is higher than the aligned state, up to 2.5 cm.

3.4. ANSYS SIMPLORER CO-SIMULATION

The WPT circuit, which works simultaneously with the coil design in the ANSYS Maxwell 3D program, was built on ANSYS Simplorer as in Fig. 13 and simulated.

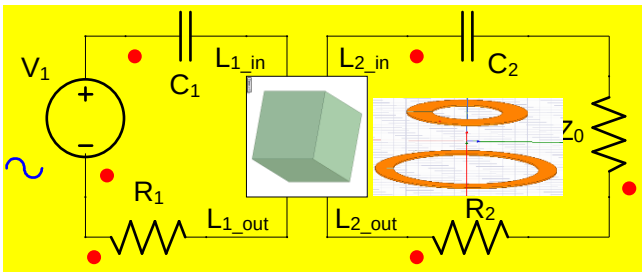

Fig. 13 WPT co-simulation circuit in Simplorer

When the circuit is simulated for 0 mm and 20 mm air gap in Ansys Simplorer, input and output powers are obtained as in Fig. 14.

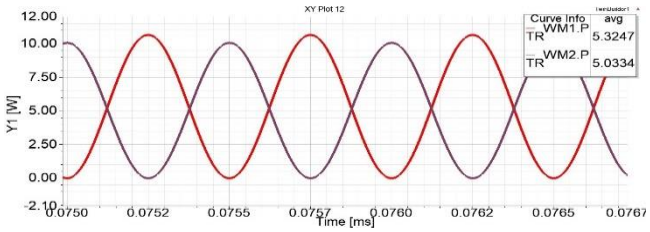

a)

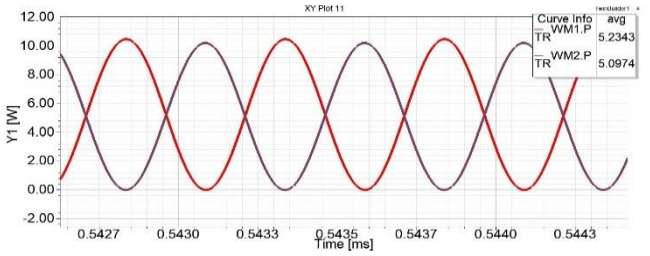

b)

Fig. 14 – a) Input (red) and output (blue) powers for 20 mm; b) input (red) and output (blue) powers for 0 mm.

The efficiency variation concerning the air gap in the aligned condition of the system with the receiver coil diameter of 5 cm and the transmitter coil diameter of 7.5 cm is shown in Fig. 15.

Since the coil sizes of the mobile telephone WPT circuits are small, it works efficiently in the low air gap. In WPT systems, after the critical air gap is exceeded, decreases in efficiency have been observed due to the weakening of the magnetic coupling.

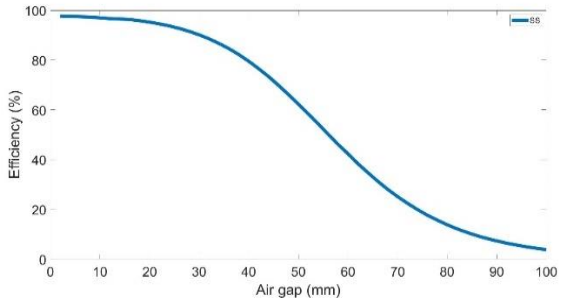

Fig. 15 – Variation of the efficiency according to the air gap

As seen in Fig. 18, after the critical air gap of 13.2 mm, an increase in the efficiency reduction rate is observed. The efficiency-frequency table obtained because of 2 different programs according to the different coupling factors, and air gap values of the WPT system is given in Table 4.

Table 4

Efficiency and frequency values in MATLAB and Ansys Simplorer

Air gap (mm), *k*		MATLAB Simulink	ANSYS Maxwell
0 mm, *k*=0.337	Frequency	0.937 MHz	0.937 MHz
	Efficiency	97.42 %	97.38 %
10 mm *k*=0.253	Frequency	0.998 MHz	0.998 MHz
	Efficiency	97 %	96.98 %
20 mm *k*=0.158	Frequency	1 MHz	1 MHz
	Efficiency	94.54 %	94.53 %

When the simulation results are examined, in both programs, close and consistent efficiency and frequency values are obtained.

4. EFFECTS ON HUMAN HEALTH

Since this WPT design is made for mobile phone charging, it is expected to be kept close to the human body. Especially a wireless charger can be placed close to the head in the house, or the human hand can remain between the coils while the mobile phone is placed on the transmitter coil for charging. In such cases, the exposure value must be below the limit values so that the electromagnetic energy absorbed by the limbs does not cause harmful effects on the tissues. If it is above the limit values, it must be detected by live object detection systems, and the system must be turned off.

Table 5

Exposure limits for 1 MHz according to ICNIRP guidelines and IEEE standards [17, 18]

Standards and Guidelines	Electric field (V/m)		Magnetic field (A/m)		Magnetic flux density (μT)		SAR (W/kg)	
İEEE (Head)	PUE	PRE	PUE	PRE	PUE	PRE	PUE	PRE
	642	1842	163	490	205	615	2	10
İEEE (Limbs)	PUE	PRE	PUE	PRE	PUE	PRE	PUE	PRE
	642	1842	900	900	1130	1130	4	20
ICNIRP (Head)	OE	GPE	OE	GPE	OE	GPE	OE	GPE
	270	135	80	21	100	27	2	10
ICNIRP (Limbs)	OE	GPE	OE	GPE	OE	GPE	OE	GPE
	270	135	80	21	100	27	4	20

To examine the effects of electromagnetic fields on human health, the scattering graphs of the magnetic field, electric field, and magnetic flux density were examined concerning IEEE standard and ICNIRP guidelines [17, 18]. Exposure limits for 1 MHz according to ICNIRP guidelines and IEEE standards are given in Table 5 [17, 18].

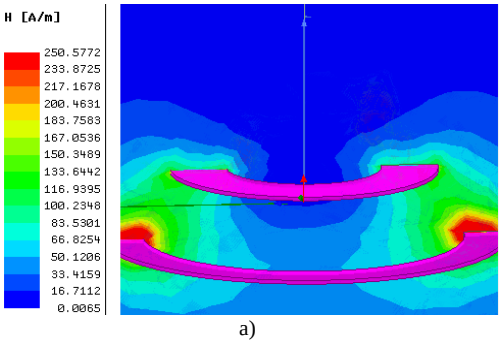

a)

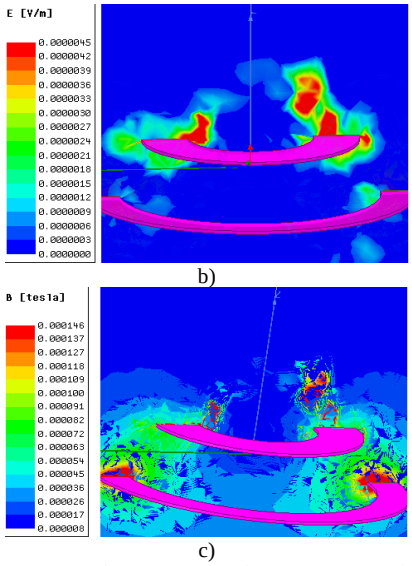

b)

c)

Fig. 16 – a) Magnetic field; b) electric field; c) magnetic flux density.

PUE is Persons in Unrestricted Environments, PRE is Persons in Restricted Environments, OE is Occupational exposure, and GPE is General Public Exposure. The magnetic field, electric field, and magnetic flux density scattered by the WPT system are shown in Fig. 16. When Fig. 16 is examined, it is seen that the electric field is a maximum of 4.5 µV/m, the magnetic flux density is a maximum of 136 µT, and the magnetic field is a maximum of 250.57 A/m.

A ferrite core (thickness: 1.5 mm, receiver diameter: 60 mm, transmitter diameter: 110 mm) can be added to the design so that the magnetic flux density does not exceed the coil limits and is concentrated around the windings. In addition, shielding (thickness: 0.5 mm, receiver diameter: 65 mm, transmitter diameter: 115 mm) can be added so that the leakage flux does not pass to the devices behind the core. Thus, the scattering will be further reduced. The magnetic flux density of the WPT system with the ferrite core and shielded is shown in Fig. 17.

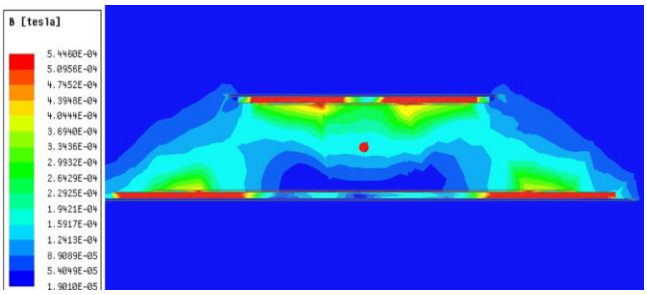

Fig. 17 – The magnetic flux density of the WPT system with ferrite core and shielded.

The variation of magnetic flux density and magnetic field on the horizontal axis from the center of the coil to the outside of the coil for different air gaps is given in Fig. 18.

From Fig. 18, it has been observed that the magnetic flux density and magnetic field are high between the inner radius of the receiver coil of 14.5 mm and the outer radius of the transmitting coil of 37.5 mm and decrease sharply outside this range.

By taking the magnetic and electric field limits values of IEEE standards and ICNIRP guidelines as a reference, the safe approach distance at which the WPT system does not adversely affect human health has been determined. When the limit values are examined according to IEEE standards, there is no harm to the head, torso, and human limbs in the restricted area. In the unrestricted area, there should be a limited approach value for the head and torso up to 3 mm, although there is no harm to the human limbs. According to ICNIRP guidelines, the limit approach value should be 3.2 cm for public exposure and 1 cm for occupational exposure.

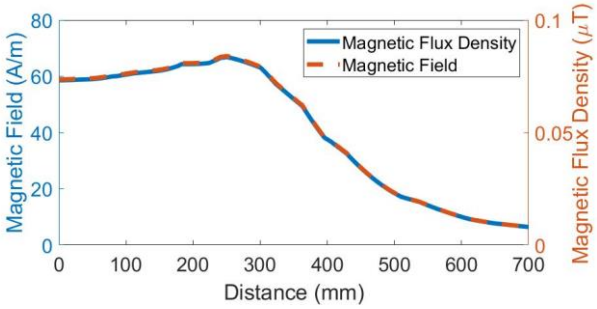

Fig 18 – Magnetic flux density and magnetic field graph according to distance from coil center to outside for different air gaps

In this study, the magnetic field, magnetic flux density, and local SAR distribution of the organs are given in Fig. 19 for examining the effect of the WPT system by placing a hand between the receiving coil and the transmitting coil and a head next to them.

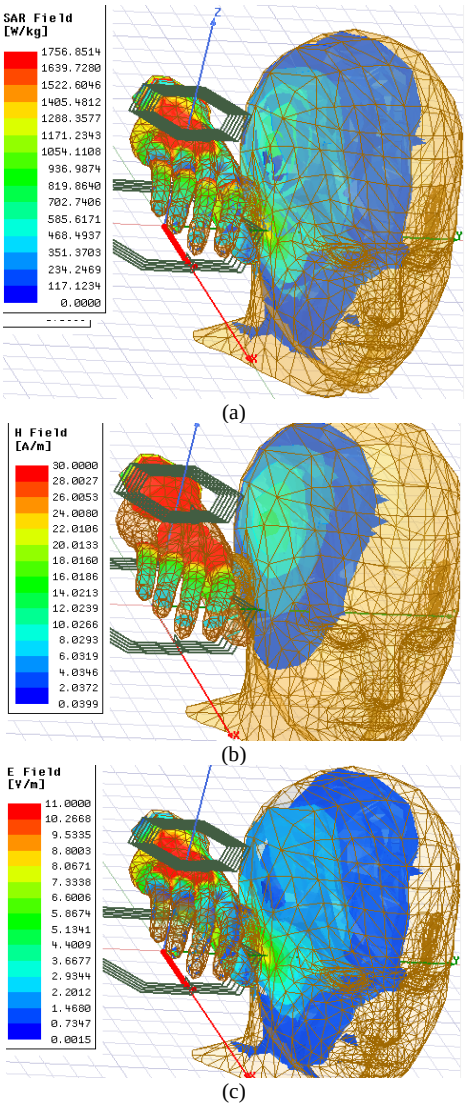

(a)

(b)

(c)

Fig. 19 – In hand and head, distribution of: a) local SAR; b) magnetic field; c) electric field.

Considering the SAR value, it was measured as a maximum of 0.1150 W/kg for the human hand and a maximum of 0.0650 W/kg for the human head. According to the ICNIRP guidelines and IEEE standards, the SAR value was determined well below the limit. When the magnetic and electric field scatterings for the human head were positioned right next to the coils, it was below the limit values. However, in the case where the human hand is placed between the receiver and the transmitter, since the magnetic field values are above the limit values, this situation harms human health. Therefore, living object detection systems are necessary for the wireless charging of mobile phones. When a living object enters between the receiver and the transmitter, the transmitter resonator must be de-energized [19].

5. **CONCLUSIONS**

Wireless power transfer has started to play an active role today and has become indispensable in every field. In this study, mathematical calculations were made for selecting the appropriate coil size so that the WPT can work efficiently in alignment and various misalignment situations in mobile phone charging. For the detailed analysis of the WPT system, simulations were carried out using multiple package programs (MATLAB, Maxwell 3D, and HFSS). It has been observed that the change of coupling factor differs for different receiver sizes according to the change of air gap and alignment status. So, the system's efficiency varies according to the air gap, alignment status, and coil size. Analyzes were made according to a fixed receiver and different transmitter coil sizes, so the optimum coil sizes were determined. It examined how the system's efficiency was affected in cases of misalignment. The maximum misalignment interval was determined at which efficient energy transfer was cut. As a result of the electromagnetic analysis, the SAR value, electric field, magnetic field, and magnetic flux density were examined. In this design, limbs placed 3 cm or more from the WPT system are below exposure limits.

However, for limbs placed closer than 3 cm or between the receiver and transmitter, the limits are exceeded. In these cases, the WPT should be stopped. In this study, analyzes were carried out to determine the optimum transmitter size and alignment tolerance for wireless charging with wide freedom of movement on the transmitter charging pad of WPT systems whose receiver size is smaller than the transmitter. In future studies, this study can be further developed for WPT systems with large transmitters and multiple small receivers.

Received on 6 September 2021

REFERENCE

1. N. Tesla, *Art of Transmitting Electrical Energy through Natural Mediums*, U.S. Patent No. 787,412 (1905).
2. M. Ishiba, J. Ishida, K. Komurasaki, Y. Arakawa, *Wireless power transmission using modulated microwave*, IEEE MTT-S International Microwave Workshop Series on Innovative Wireless Power Transmission: Tech., Sys., and App., pp. 51–54 (2011).
3. K.J. Duncan, *Laser based power transmission: Component selection and laser hazard analysis*, IEEE PELS Workshop on Emerging Technologies: Wireless Power Transfer, pp. 100–103 (2016).
4. P.C. Ghosh, P.K. Sadhu, S. Das, *A Hıgh-Performance Z-Source Resonant Inverter for Contactless Power Transfer*, Rev. Roum. Sci. Techn. – Électrotechn. et Énerg., **62**, *3*, pp. 282–287 (2017).
5. E. Abramov, M.M. Peretz, *Multi-loop control for power transfer regulation in capacitive wireless systems by means of variable matching networks*, IEEE Journal of Emerging and Selected Topics in Power Electronics, **8**, *3*, pp. 2095–2110 (2020).
6. M. Budhia, G.A. Covic, J.T. Boys, *Design and Optimization of Circular Magnetic Structures for Lumped Inductive Power Transfer Systems*, IEEE Transactions on Power Electronics, **26**, *11*, pp. 3096–3108 (2011).
7. T. Imura, Y. Hori, *Maximizing Air Gap and Efficiency of Magnetic Resonant Coupling for Wireless Power Transfer Using Equivalent Circuit and Neumann Formula*, IEEE Transactions on Industrial Electronics, **58**, *10*, pp. 4746–4752 (2011).
8. M. Stanculescu, M. Iordache, D. Nıculae, L. Bobaru, V. Bucată, *Algorithm for computing s parameters and their use for studying efficiency of electromagnetic energy wireless transfer systems*, Rev. Roum. Sci. Techn. – Électrotechn. et Énerg., **63**, *2*, pp. 138–144 (2018).
9. N. Bekiroglu, A. Ağçal, S. Ozcira, *Validation of wireless power transfer by using a 3D representation of magnetically coupled resonators considering peak efficiency*, J. of Magnetıcs, **23**, *1*, pp.11–17, (2018).
10. G. Zulauf, J.M. Rivas-Davila, *Single-Turn Air-Core Coils for High-Frequency Inductive Wireless Power Transfer*, IEEE Transactions on Power Electronics, **35**, *3*, pp. 2917–2932 (2020).
11. Y. Zhang, S. Chen, X. Li, Z. She, F. Zhang, Y. Tang, Coil *Comparison and Downscaling Principles of Inductive Wireless Power Transfer Systems*, IEEE PELS Workshop on Emerging Technologies: Wireless Power Transfer (WoW), 2020, pp. 116–122.
12. E. Aydin, M.T. Aydemir, *A 1-kW wireless power transfer system for electric vehicle charging with hexagonal flat spiral coil*, Turkish Journal of Electrical Engineering and Computer Sciences, **29**, *5*, pp. 2346–2361 (2021).
13. Z. Luo, X. Wei, *Analysis of square and circular planar spiral coils in wireless power transfer system for electric vehicles*, IEEE Transactions on Industrial Electronics, **65**, *1*, pp. 331–341 (2017).
14. K. Song, G. Yang, Y. Guo, Y. Lan, S. Dong, J. Jiang, C. Zhu, *Design of DD coil with high misalignment tolerance and low EMF emissions for wireless electric vehicle charging systems*, IEEE Transactions on Power Electronics, **35**, *9*, pp. 9034–9045 (2020).
15. A. Agcal, S. Ozcira, K. Toraman, *Comparison of compensating topologies in two coils resonant wireless power transfer system*, Journal of Engineering Research, online first article, 2022.
16. H.A. Wheeler, *Simple Inductance Formulas for Radio Coils*, Proceedings of the Institute of Radio Engineers, **16**, *10*, pp. 1398–1400 (1928).
17. *IEEE Standard for safety levels with respect to human exposure to electric, magnetic, and electromagnetic fields, 0 Hz to 300 GHz*, IEEE Std C95.1-2019, **4**, pp. 1–312 (2019).
18. ICNIRP, *Guidelines for limiting exposure to electromagnetic fields (100 kHz to 300 GHz)*, Health Physics, **118**, *5*, pp. 483–524 (2020).
19. J. Lu, G. Zhu, C.C. Mi, *Foreign Object Detection in Wireless Power Transfer Systems*, IEEE Trans. on Industry Applications, **58**, *1*, pp. 1340–1354 (2022).